

State-dependent electrostatic interactions of S4 arginines with E1 in S2 during Kv7.1 activation

Dick Wu, Kelli Delaloye, Mark A. Zayzman, Ali Nekouzadeh, Yoram Rudy, and Jianmin Cui

Department of Biomedical Engineering and Cardiac Bioelectricity and Arrhythmia Center, Washington University, St. Louis, MO 63130

The voltage-sensing domain of voltage-gated channels is comprised of four transmembrane helices (S1–S4), with conserved positively charged residues in S4 moving across the membrane in response to changes in transmembrane voltage. Although it has been shown that positive charges in S4 interact with negative countercharges in S2 and S3 to facilitate protein maturation, how these electrostatic interactions participate in channel gating remains unclear. We studied a mutation in Kv7.1 (also known as KCNQ1 or KvLQT1) channels associated with long QT syndrome (E1K in S2) and found that reversal of the charge at E1 eliminates macroscopic current without inhibiting protein trafficking to the membrane. Pairing E1R with individual charge reversal mutations of arginines in S4 (R1–R4) can restore current, demonstrating that R1–R4 interact with E1. After mutating E1 to cysteine, we probed E1C with charged methanethiosulfonate (MTS) reagents. MTS reagents could not modify E1C in the absence of KCNE1. With KCNE1, (2-sulfonatoethyl) MTS (MTSES)[–] could modify E1C, but [2-(trimethylammonium)ethyl] MTS (MTSET)⁺ could not, confirming the presence of a positively charged environment around E1C that allows approach by MTSES[–] but repels MTSET⁺. We could change the local electrostatic environment of E1C by making charge reversal and/or neutralization mutations of R1 and R4, such that MTSET⁺ modified these constructs depending on activation states of the voltage sensor. Our results confirm the interaction between E1 and the fourth arginine in S4 (R4) predicted from open-state crystal structures of Kv channels and reveal an E1–R1 interaction in the resting state. Thus, E1 engages in electrostatic interactions with arginines in S4 sequentially during the gating movement of S4. These electrostatic interactions contribute energetically to voltage-dependent gating and are important in setting the limits for S4 movement.

INTRODUCTION

The opening and closing of voltage-gated ion channels in response to changes in membrane potential provide the molecular basis for electrical signaling in neurons and cardiac myocytes (Hille, 2001). Voltage-gated potassium (Kv) channels terminate the action potential and are formed by the coassembly of four identical subunits, each consisting of six transmembrane helices. The first four helices (S1–S4) form the voltage-sensing domain (VSD), and S5–S6 form the pore domain. Conserved basic residues in S4 of the VSD can sense the electric field across the membrane. Membrane depolarization induces a conformational change in the VSD, such that S4 moves outwards. This conformational change causes the activation gate to open, allowing passage of potassium ions through the conduction pore (Tombola et al., 2006).

Conserved acidic residues in S1–S3 of the VSD and phospholipids in the membrane have been shown to provide stabilizing electrostatic interactions to the highly charged S4 segment traversing the hydrophobic

membrane environment (Papazian et al., 1995; Tiwari-Woodruff et al., 1997; Freites et al., 2005; Schmidt et al., 2006; Long et al., 2007; Zhang et al., 2007; Xu et al., 2008; Krepkiy et al., 2009). Previous intragenic suppression studies of charged residues in the VSD suggest that electrostatic interactions between the third and fourth arginines in S4 (R3 and R4) and the first glutamate in S2 (E1) (Fig. 1 A) are important for the maturation of Shaker K⁺ channels (Papazian et al., 1995; Tiwari-Woodruff et al., 1997; Zhang et al., 2007). The crystal structure of the Kv1.2 channel shows a close proximity between E1 and R4 in the open state of the channel, suggesting that they form a salt bridge (Long et al., 2005, 2007). Inspired by these findings, computational models describing the gating process of voltage-dependent channels have been proposed with an assumption that electrostatic interactions between arginines in S4 and negatively charged residues in the rest of the VSD contribute to channel gating (Lecar et al., 2003; Silva et al., 2009). However, experimental results confirming the existence of electrostatic interactions in different states

Correspondence to Jianmin Cui: jcui@biomed.wustl.edu

Abbreviations used in this paper: Kv, voltage-gated potassium; MTS, methanethiosulfonate; MTSAC, [2-(aminocarbonyl)ethyl] MTS; MTSES, (2-sulfonatoethyl) MTS; MTSET, [2-(trimethylammonium)ethyl] MTS; VSD, voltage-sensing domain; WT, wild-type.

are still lacking. Although disulfide bond and metal bridging studies have increasingly constrained the resting conformation of S4 (Campos et al., 2007; Haitin et al., 2008), electrostatic interactions in the resting state of the VSD are not known.

Kv7.1 is a Kv channel that coassembles with KCNE1 (also known as minK) in the heart to form the I_{Ks} channel, an essential channel for the termination of cardiac action potentials and the maintenance of normal heart rhythm (Barhanin et al., 1996; Sanguinetti et al., 1996; Nerbonne and Kass, 2005). The E160K (E1K) missense mutation in S2 of Kv7.1 has been previously implicated in inherited long QT syndrome, predisposing affected individuals to syncope, ventricular arrhythmias, and sudden cardiac death (Splawski et al., 2000). Using this mutant as a starting point, we used charge reversal mutagenesis to determine that this residue is likely involved in electrostatic interactions with S4. Combining charge reversal mutagenesis with methanethiosulfonate (MTS) modification probing of the E1C mutant shows that E1 interacts electrostatically with arginines in S4 in both the resting and activated states during Kv7.1+KCNE1 channel gating. We found that E1 interacts with R1 only in the resting state. Upon activation of the VSD, R1 becomes distal to E1 and R4 interacts with E1. These results indicate that S4 arginines participate in sequential electrostatic interactions with E1 during voltage-dependent activation of Kv7.1, a finding also supported by disulfide cross-linking studies in NaChBac channels (DeCaen et al., 2008, 2009). These interactions provide an approximation of the limits for the movement of S4 during gating.

MATERIALS AND METHODS

Mutagenesis and oocyte preparation

Mutations were made using PCR (Shi et al., 2002). Kv7.1 (provided by S. Goldstein, University of Chicago, Chicago, IL) and KCNE1 (provided by S. Nakanishi, Osaka Bioscience Institute, Osaka, Japan) were subcloned into the HindIII/XbaI cloning sites of pcDNA3.1⁺ vectors (Invitrogen). Mutagenesis was performed using overlap extension amplification with high-fidelity PCR. DNA sequencing confirmed the accuracy of the mutations. mRNA was made using the mMessage mMachine T7 polymerase kit (Applied Biosystems). Defolliculated stage V–VI *Xenopus* oocytes were injected with 46 ng/oocyte of mRNA. Injected oocytes were incubated at 18°C in ND96 solution (in mM: 96 NaCl, 2 KCl, 1.8 CaCl₂, 1 MgCl₂, and 5 HEPES, pH 7.60) for 3–5 d for channel expression.

Electrophysiology

Oocyte current recordings were obtained with the two-microelectrode voltage clamp technique (Deng et al., 2004). Microelectrodes were pulled from glass capillary tubes and filled with 3 M KCl. Oocytes were constantly superfused with ND96. The membrane potential was clamped using a voltage clamp amplifier (Dagan CA-1B; Dagan Corporation). Data acquisition was controlled using PULSE/PULSEFIT software (HEKA). Data were analyzed using IGOR Pro 6 (WaveMetrics). The Boltzmann function was used to fit current–voltage relationships, where: normalized $I_{tail} = P_O = 1/[1 + \exp((V_{1/2} - V_t)/k)]$.

[2-(Trimethylammonium)ethyl] MTS (MTSET)⁺, (2-sulfo-natoethyl) MTS (MTSES)⁻, and [2-(aminocarbonyl)ethyl] MTS (MTSACE; Toronto Research Chemicals) were made into aliquots of 100-mM stock solution. Aliquots were thawed and diluted into ND96 immediately before use.

Biochemistry

Intact oocytes expressing the protein of interest were incubated in a 1-mg/ml solution of Sulfo-NHS-SS-Biotin (Thermo Fisher Scientific) to label membrane proteins. Oocytes were washed to remove unbound biotin and homogenized. The lysates were incubated with NeutrAvidin beads (Thermo Fisher Scientific) to pull out biotin-bound proteins. The NeutrAvidin beads were collected via centrifugation and washed thoroughly. Lysates and beads were heated to 60°C in SDS-PAGE loading buffer. After electrophoresis, samples were Western blotted with a 1:500 dilution of Kv7.1 primary (Santa Cruz Biotechnology, Inc.) and a 1:5,000 dilution of goat anti-rabbit secondary antibody (Santa Cruz Biotechnology, Inc.). Anti-G_B antibody was used to probe for control proteins (Santa Cruz Biotechnology, Inc.).

Electrostatic calculations and structural modeling

A 3-D structure of the Kv7.1 channel was derived based on its homology with the Kv1.2 channel, as described previously (Silva et al., 2009). Movement of the S3b–S4 complex was assumed to be the major conformational change during gating. Five degrees of freedom were assumed for the S3b–S4 motion (three translational and two rotational), and one million conformations were generated for different combinations of these degrees of freedom. Conformations with steric overlap were eliminated. The electrostatic energies of the remaining conformations for various membrane potentials were computed considering the Debye–Hückel length and screening effect of electrolytes. The steady-state probability distribution of the protein among these conformations was calculated using Boltzmann weights:

$$w_i = e^{-\frac{\varphi_i}{kT}},$$

where φ_i is the potential energy of the i_{th} conformation.

The Kv7.1 template structure was based on the Kv1.2 open-state crystal structure. The channel was assumed to be in the activated state within 2-Å inward (z direction) displacement of the S3b–S4 complex; for movement >2 Å, the channel was assumed to be in a resting state. Based on this hypothesis, channels in an allowable conformation were determined to be either activated or at rest.

Online supplemental material

We have included data in Fig. S1 for MTSES⁻ and MTSET⁺ application to various control constructs demonstrating that MTS reagents do not modify these channels. Fig. S1 is available at <http://www.jgp.org/content/full/jgp.201010408/DC1>.

RESULTS

Kv7.1 is sensitive to charge perturbations at the E1 position

Like most voltage-dependent channels, Kv7.1 contains two conserved glutamates in S2 (E1 and E2) and a series of arginines in S4 (R1, R2, etc.) (Fig. 1 A). However, Kv7.1 has a glutamine (Q3) at what is the third arginine position and a histidine (H5) at what is the fifth arginine position in Shaker. We found that E1K or E1K+KCNE1 generates current indistinguishable from background

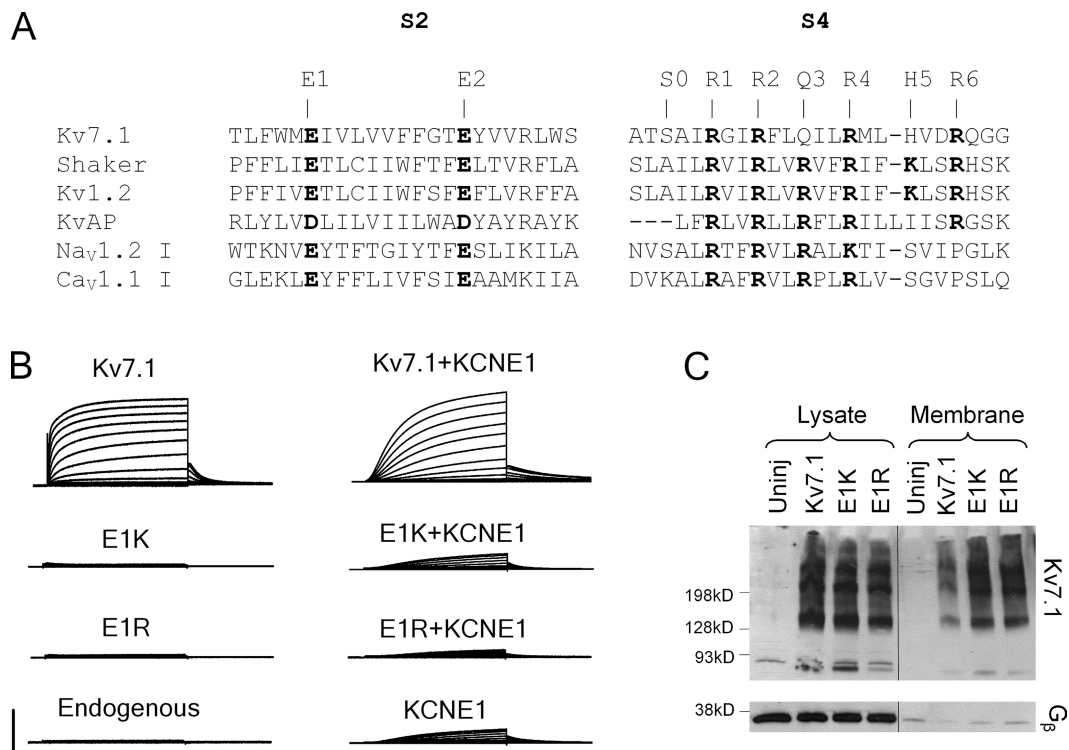


Figure 1. Sequence alignment of S2 and S4 from various voltage-dependent ion channels and proteins. (A) Conserved negatively charged residues in S2 and positively charged residues in S4 are in bold. (B) Currents generated from WT, E1K, and endogenous channels. Oocytes were held at -80 mV, depolarized from -80 to $+60$ mV for 5 s, and repolarized at -40 mV for 3 s. Scale, 4 μ A for all except Kv7.1+KCNE1 (20 μ A); 2 s for all currents in this and subsequent figures. (C) Western blot probing for Kv7.1 and G_{β} in the whole cell lysate and biotinylated membrane fraction from oocytes. G_{β} is a cytoplasmic protein. Black lines indicate that intervening lanes have been spliced out.

current expressed by native oocyte channels without or with KCNE1 (<0.5 or <2 μ A, respectively), and much smaller than wild-type (WT) Kv7.1 or WT Kv7.1+KCNE1 currents (Fig. 1 B), suggesting that E1K channels themselves do not generate any current. A similar charge reversal mutation, E1R, exhibits an identical phenotype to E1K (Fig. 1 B). In contrast to Shaker channels (Papazian et al., 1995; Tiwari-Woodruff et al., 1997), Western blots of biotinylated surface Kv7.1 proteins show that E1K/R can assemble as a homomultimer and traffic to the membrane (Fig. 1 C). Bands corresponding to Kv7.1 tetramer (280 kD), trimer (210 kD), dimer (140 kD), and monomer (70 kD) are visible for WT channels and E1K/R mutants both in lysate and membrane. Probing for G_{β} protein in the same blot shows that G_{β} is only present in the lysate, but not the membrane, confirming that intracellular proteins were not biotinylated. When E1 was conservatively mutated to the negatively charged aspartate or mutated to the electrically neutral glutamine, cysteine, or alanine, all formed functional channels, although E1A reduced current (Fig. 2 A). Neutralizing mutations all shifted the G-V relationship rightwards (Fig. 2 B), suggesting that removal of the negative charge at E1 hinders channel activation. Only a positive charge at E1 completely abolished current. These results suggest that the loss of current is caused

by the inability of E1K/R channels to open, possibly through disruption of electrostatic interactions involving E1 and not due to a trafficking defect.

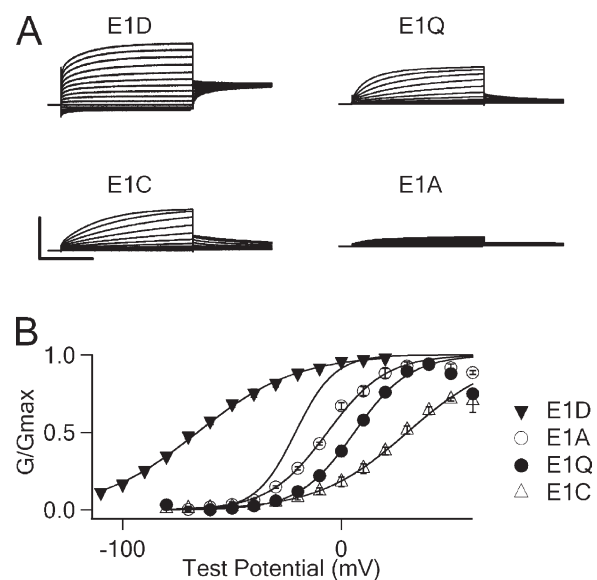


Figure 2. Currents from various E1 mutations to negative or neutral residues in Kv7.1 obtained using the protocol in Fig. 1 B. (A) Scale, 4 μ A. (B) G-V relationship from mutations in A. Gray line represents WT Kv7.1. Error bars represent standard error of the means.

E1 interacts electrostatically with S4 arginines

Inspecting the sequence of Kv7.1 and KCNE1 reveals that the arginines in the S4 segment of Kv7.1 are the only positively charged residues in the membrane-spanning segments. If repulsion between E1K/R and these arginines inhibits channel activation, we hypothesized that pairing E1R with glutamate point mutations in S4 (R1E, R2E, Q3E, etc.) may restore electrostatic attraction and recover channel function. Indeed, E1R paired with R1E, R2E, Q3E, or R4E generated currents significantly larger than currents from E1R alone (Fig. 3, A and B). These four residues correspond to positive charges in Shaker that contribute the bulk of the gating charge (Aggarwal and MacKinnon, 1996; Seoh et al., 1996). S0E, H5E, and R6E that flank these four residues could not rescue any current (Fig. 3 B). These data suggest that E1 interacts electrostatically not only with R4, but also with R1 and R2. Q3 may also be positioned to interact with E1 through hydrogen bonding in native channels. Restoring electrostatic attractions between specific residues and E1R allows S4 to occupy an activated conformation so that channels can open, albeit with properties different

from WT channels. All the rescued currents except for E1R/Q3E changed instantaneously in response to voltages from -120 to $+60$ mV (Fig. 3 A). These currents have reversal potentials that approach the K^+ equilibrium potential (~ 80 – 90 mV) and can be blocked by the Kv7.1 pore-blocker chromanol 293B (Fig. 4), confirming that these are K^+ currents carried through the conduction pore of constitutively open channels.

We repeated these experiments with KCNE1 coexpression to determine if KCNE1 affects E1–S4 interactions. Overall, a similar trend of E1 interactions with S4 arginines was observed in the presence of KCNE1 (Fig. 3, C and D), although E1R/R1E+KCNE1 did not generate current. However, additional experiments described below confirm that R1 is proximal to E1 in the presence of KCNE1.

Electropositive environment around E1 formed by S4 arginines

To more directly determine whether E1 engages in electrostatic interactions with S4, we used the mutation E1C and tested its reactivity with MTS reagents in the

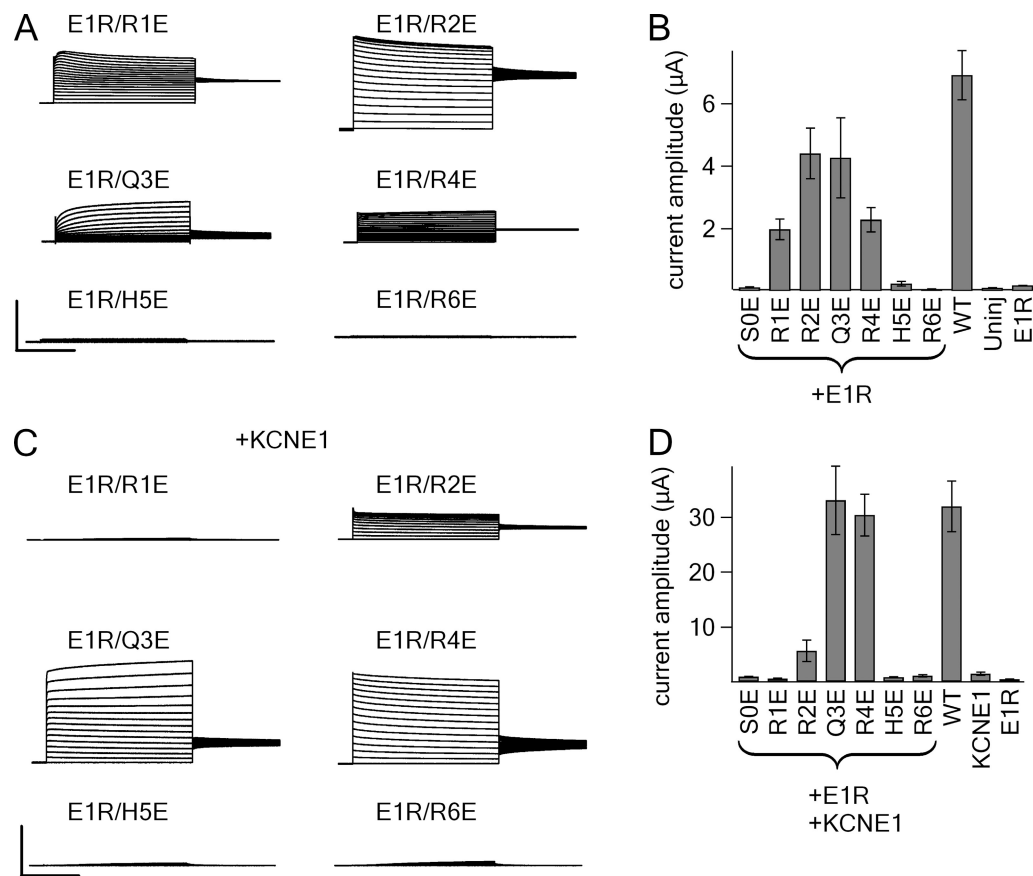


Figure 3. S4 mutations to glutamate restore E1R current. (A) Currents were recorded from double mutations shown using the voltage protocol as in Fig. 1 B. Scale, 6 μ A. (B) Peak current amplitudes in A were averaged for each mutation. Error bars represent standard error of the means. (C) Current from E1R paired with S4 residues mutated to glutamate coexpressed with KCNE1. Scale, 20 μ A. (D) Peak current amplitudes in C were averaged for each mutant. Error bars represent standard error of the means.

background of S4 arginine mutations. MTS reagents covalently modify cysteine residues that are exposed to solution (Larsson et al., 1996; Yang et al., 1996). The progress of the reaction can be monitored if modification causes a change in the macroscopic current. Charged residues located proximal to an exposed cysteine have been shown to influence the modification rate by charged MTS reagents through electrostatic forces (Elinder et al., 2001), which provided us the basis to probe the electrostatic environment around E1C. We superfused oocytes expressing E1C channels with 400 μ M MTSES⁻ or MTSET⁺, but we observed no change in current (Fig. 5 A). This finding suggests that E1C is not exposed to the extracellular milieu and cannot be modified. We cannot dismiss the possibility that E1C was modified but did not produce functional changes, but this is unlikely because the E1 position is sensitive to charge-perturbing mutations (Figs. 1 and 2).

When we coexpressed E1C with KCNE1, MTSES⁻ modified E1C to increase current amplitude threefold

(Fig. 5 B). It is likely that KCNE1 induced a conformational change, such that E1C became at least partially exposed to the extracellular solution. Yet, the application of MTSET⁺ to E1C+KCNE1 did not cause an appreciable change in the current. Subsequent application of MTSES⁻ after washout of MTSET⁺ increased current amplitude threefold, indicating that MTSET⁺ had not modified E1C+KCNE1. The application of neutral MTSACE to E1C+KCNE1 induced only minor changes in current amplitude; however, subsequent application of MTSES⁻ did not further change current amplitude (Fig. 5 B). Our interpretation is that MTSACE modified E1C+KCNE1 but caused minimal functional changes. From these experiments, we conclude that E1C experiences a strong, positive electric field, which repels MTSET⁺, preventing it from modifying E1C. On the other hand, MTSES⁻ and MTSACE can access and modify E1C.

If the positive electrostatic environment around E1 is created by arginines in S4, mutating these arginines to

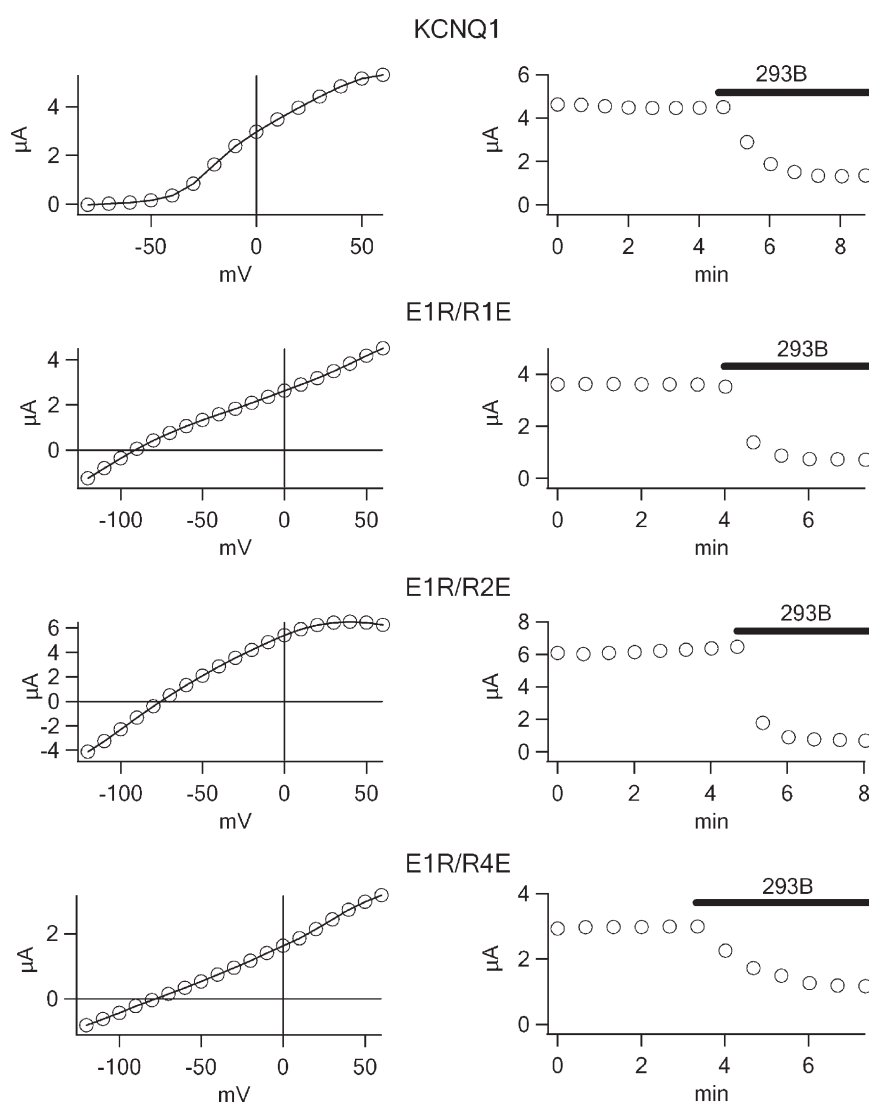


Figure 4. I-V relationships of various mutants generating constitutive current (left). Protocol same as Fig. 1 B. (Right) Block of current by KCNQ1 pore blocker chromanol 293B (100 μ M) while pulsing to +40 mV for 5 s, repolarizing at -40 mV for 3 s, and holding at -80 mV for 32 s.

negative or neutral residues would reduce the electropositivity of the E1C environment, thereby changing its modification by charged MTS reagents. We paired R4E with E1C coexpressed with KCNE1 and determined if MTSET⁺ could now modify the channel. Indeed, MTSET⁺ modified E1C/R4E+KCNE1 to elicit a 50% increase in current amplitude (Fig. 6 A), indicating that R4E contributes to the electrostatic environment of E1C. Interestingly, MTSES⁻ could still modify this channel to cause a 50% increase in current (Fig. 6 A). The ability for both reagents to modify E1C/R4E+KCNE1 suggests that the environment around E1C is not solely electropositive or electronegative in the background of R4E. We hypothesize that the motion of S4 brings different arginines into position to affect the E1 environment at different states.

From the crystal structure of the Kv1.2 and Kv1.2/2.1 chimera channels, E1 and R4 may form a salt bridge in the open state (Long et al., 2005, 2007). Currently, there is no crystal structure capturing a voltage-gated channel in the resting state. Although it is often assumed that electrostatic interactions between E1 and R1 stabilize the VSD in the resting state (Lecar et al., 2003; Silva et al., 2009), experimental evidence supporting this claim is lacking. The above paired charge reversal experiments suggest that R1 interacts with E1 (Fig. 3, A and B). Consistent with this result, when we neutralized R1 (R1Q), MTSET⁺ modified E1C to decrease E1C/R1Q+KCNE1 current by 50% (Fig. 6 B), indicating that R1 also contributes to the electrostatic environment of E1. MTSES⁻ could still modify the channel (Fig. 6 B), indicating that other arginines

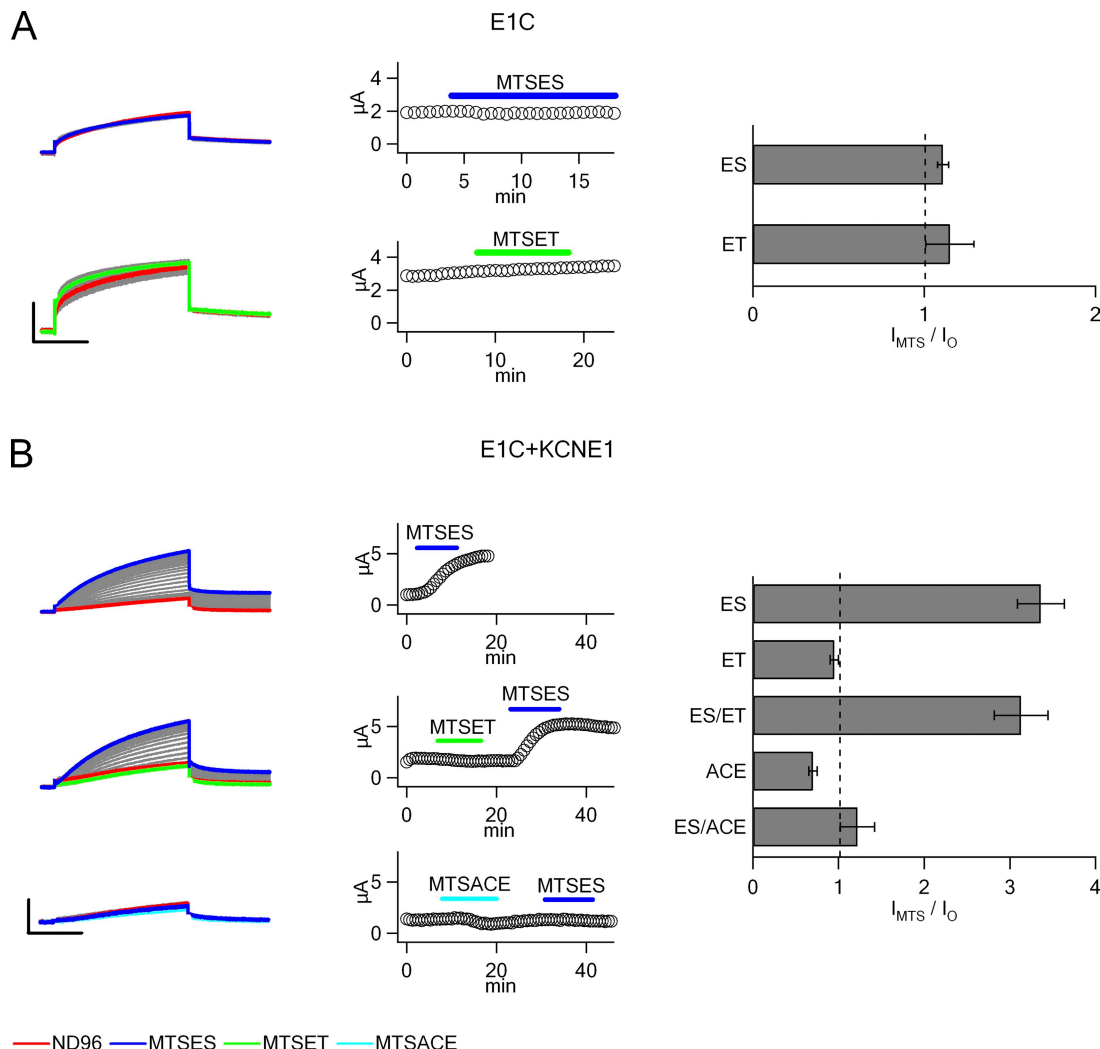


Figure 5. E1C currents after superfusion of MTSES⁻ or MTSET⁺. (A; left) Oocytes were repeatedly held at -80 mV for 32 s, depolarized at $+40$ mV for 5 s, and repolarized at -40 mV for 3 s. Scale, 2 μ A. (Middle) Peak current amplitudes at $+40$ mV plotted against time. (Right) Normalized peak current amplitude after various MTS treatments. Error bars represent standard error of the means. (B; left) E1C+KCNE1 currents after superfusion of MTSES⁻, MTSET⁺, or MTSACE. Same protocol used as in A. Scale, 3 μ A. (Middle) peak current amplitudes at $+40$ mV plotted against time. (Right) Normalized peak current amplitude after various MTS treatments. Error bars represent standard error of the means.

may be proximal to E1C at different states (see below). This result also confirms that R1 is proximal to E1 in the presence of KCNE1, even though paired charge reversal experiments could not conclusively show this interaction (Fig. 3, C and D).

We found that E1C/R1E channels both with and without KCNE1 were constitutively open and unresponsive to MTSET⁺ or MTSES⁻ (Fig. 7 A). In WT Kv7.1, R1 may be located in the transmembrane electrical field at hyperpolarizing potentials (Nakajo and Kubo, 2007; Rocheleau and Kobertz, 2008). Therefore, negatively charged R1E would experience an outward force at hyperpolarizing potentials, making it energetically unfavorable for S4 to reside in the resting state. In light of this hypothesis, we introduced a positive charge at Q3 (Q3R), a residue known to reside in the electric field in Shaker channels (Larsson et al., 1996), in an attempt to stabilize the resting state at hyperpolarizing potentials. As hypothesized, the E1C/R1E/Q3R channels recovered volt-

age dependence both in the absence and presence of KCNE1 (Fig. 7 B), allowing us to repeat the MTS experiments described above with this construct. We found that both MTSET⁺ and MTSES⁻ changed current amplitude (Fig. 7 C), similar to the effect observed in E1C/R1Q+KCNE1 (Fig. 6 B). Although MTSET⁺ modification reduced current amplitude, it did not alter the G-V relationship (Fig. 7 C). Channels modified by MTSET⁺ likely remain closed, thereby reducing the population of channels available to open and contribute to the macroscopic current. After MTSET⁺ modification, we believe a positive charge at E1C attracts R1E to stabilize the resting state and repulses R4 to destabilize the activated state, preventing channel activation. On the other hand, MTSES⁻ modification causes a leftward shift in the G-V (Fig. 7 C), perhaps due to repulsion between a negative charge at E1C and R1E to destabilize the resting state, and attraction between a negative charge at E1C and R4 to favor the activated state.

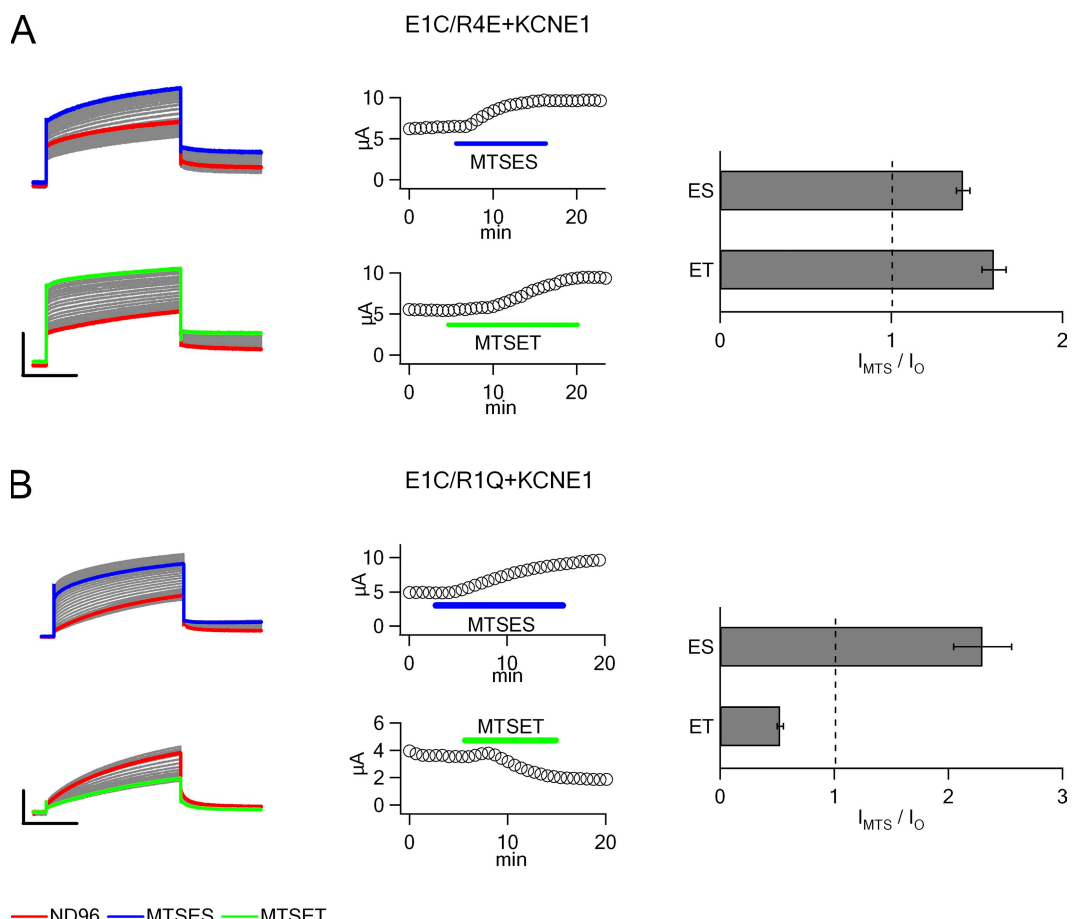


Figure 6. E1C/R4E+KCNE1 currents after superfusion of MTSES⁻ or MTSET⁺. (A, left) The same pulse protocol was used as in Fig. 5 A. Scale, 5 μA . (Middle) Peak current amplitudes plotted against time. (Right) Normalized peak current amplitude after various MTS treatments. Error bars represent standard error of the means. (B; left) E1C/R1Q+KCNE1 currents after superfusion of MTSES⁻ or MTSET⁺. The same pulse protocol was used as in A. Scale: top, 5 μA ; bottom, 2 μA . (Middle) Peak current amplitudes plotted against time. (Right) Normalized peak current amplitude after various MTS treatments. Error bars represent standard error of the means.

R1 proximity to E1 is state dependent

To verify that R1 interaction with E1 is dependent on the state of channel gating, we compared MTSET⁺ modification of the E1C/R1E/Q3R+KCNE1 channels when the membrane potential was held at -80 or $+40$ mV with the voltage sensor residing predominantly at the resting or activated state, respectively. The application of MTSET⁺ at -80 mV resulted in a decreased current amplitude upon resumption of test pulses (Fig. 8 A). Subsequent application of MTSET⁺ did not further decrease current, indicating that most of the available E1C sites had been modified. In contrast, when MTSET⁺ was applied at $+40$ mV, the current was unchanged upon resumption of test pulses (Fig. 8 A). Further application of MTSET⁺ resulted in a sharp decline in current ampli-

tude, confirming that few E1C sites had been modified at $+40$ mV. These results suggest that R1E influences E1C only at hyperpolarizing voltages when the VSD is primarily at the resting state.

We further measured the state dependence of MTSET⁺ modification at different holding potentials (-100 to $+20$ mV), while pulsing to $+80$ mV periodically to check the result of modification (Fig. 8 B). The decay of current at $+80$ mV after MTSET⁺ treatment was fit with a single exponential to obtain the modification rate ($1/\tau$) at each holding potential. The rate of modification decreased as the holding potential increased (Fig. 8 B), indicating that E1C is more readily accessible by MTSET⁺ in the resting state of the voltage sensor. The rate of modification versus holding potentials was fit well by

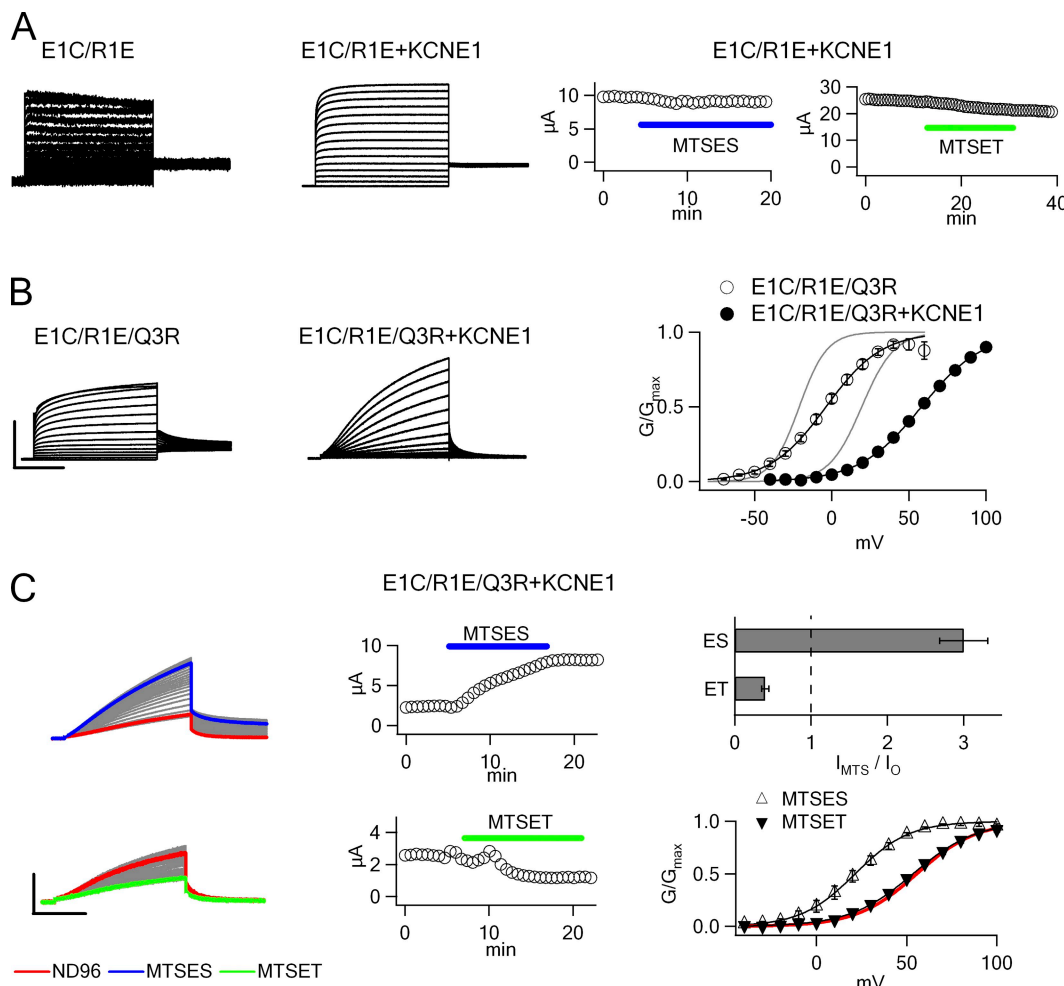


Figure 7. Currents from E1C/R1E and E1C/R1E+KCNE1. (A, left) Same protocol used as in Fig. 1 B. (Right) E1C/R1E+KCNE1 currents after superfusion of MTSES⁻ or MTSET⁺. (B; left) Currents from E1C/R1E/Q3R and E1C/R1E/Q3R+KCNE1. Same protocol as in A. (Right) G-V relationships from E1C/R1E/Q3R with or without KCNE1 were plotted with G-V relationships of WT Kv7.1 (left gray line) or WT Kv7.1+KCNE1 (right gray line). Error bars represent standard error of the means. Scale: E1C/R1E, 0.7 μ A; E1C/R1E+KCNE1, 12 μ A; E1C/R1E/Q3R, 1 μ A; E1C/R1E/Q3R+KCNE1, 5 μ A. (C; left) E1C/R1E/Q3R+KCNE1 currents after superfusion of MTSES⁻ or MTSET⁺. Same protocol as in Fig. 5 A. Scale: top, 5 μ A; bottom, 2 μ A. (Middle) Peak current amplitudes plotted against time. Error bars represent standard error of the means. (Right; top) Normalized peak current amplitude after various MTS treatments. (Right; bottom) G-V relationships before and after MTS treatment. Red line indicates the G-V before MTS treatment. Error bars represent standard error of the means.

a summation of two Boltzmann distributions with $V_{1/2,a}$ of -75 mV and slope_a of 5 mV, and $V_{1/2,b}$ of 8 mV and slope_b of 8 mV (Fig. 8 B), suggesting that S4 may move in two sequential steps. This feature of S4 movement was shown by gating current and fluorescence studies in Shaker channels (Bezanilla et al., 1994; Baker et al., 1998) and suggested by models of Shaker and Kv7.1 gating (Zagotta et al., 1994; Silverman et al., 2003; Silva and Rudy, 2005; Silva et al., 2009). Thus, at extreme hyperpolarizing potentials, S4 likely occupies a deep resting conformation with R1 situated close to E1. At intermediate hyperpolarizing potentials, S4 primarily resides in a resting conformation where R1 is located farther from E1, thereby reducing the efficacy of MTSET⁺ modification of E1C. Further depolarization increases the occupancy of S4 in the activated conformation, where R1 moves into the extracellular space and has limited impact on the E1 electrostatic environment. Due to the lack of gating current and fluorescence data on

Kv7.1 channels, these experimental results offer the first glimpse into voltage sensor movement in Kv7.1 channels.

Structural model of Kv7.1 derived from electrostatic calculations

To illustrate these results, we adopted a model recently developed for the voltage sensor movement during Kv7.1 channel gating by combining molecular dynamics simulations and Poisson-Boltzmann continuum electrostatic calculations (Silva et al., 2009). Instead of assuming a helical screw motion of S4 as in the original model, in this study S3b and S4 move together and with more degrees of freedom (see Materials and methods). Moving from the activated state to an intermediate resting state and finally to the deep resting state, S3b–S4 translates 12 Å inward toward the intracellular space, 7 Å toward the pore region, and 4 Å tangential to the pore (parallel to the membrane); it also rotates 130° counterclockwise (observed from extracellular space)

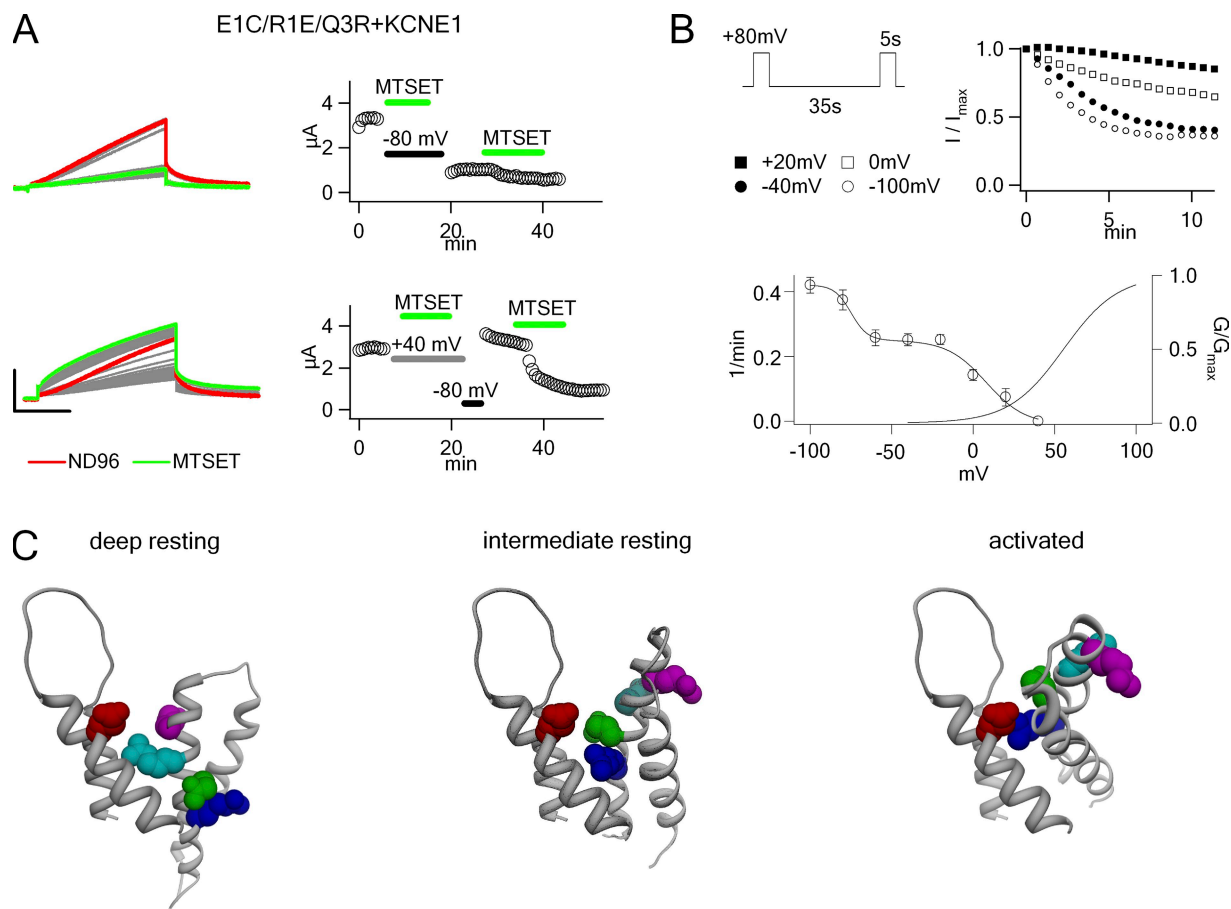


Figure 8. E1C/R1E/Q3R+KCNE1 currents after superfusion MTSET⁺. (A; left) Oocytes were held at either -80 or $+40$ mV, with perfusion of MTSET⁺ as indicated, followed by resumption of test pulses. Scale, 0.7 μ A. (Right) Peak current amplitudes plotted against time. (B) Voltage dependence of MTSET⁺ modification. (Left) Pulse protocol used. The holding potential was varied. (Middle) Time course of MTSET⁺ modification at different holding potentials. (Right) Rates of MTSET⁺ modification plotted against holding potential. The rates were fit with a double Boltzmann function (see Materials and methods) with $V_{1/2,a}$ of -75 mV and slope_a of 5 mV, and $V_{1/2,b}$ of 8 mV and slope_b of 8 mV. Error bars represent standard error of the means. G-V before MTS modification was also plotted. (C) Structures of the deep resting, intermediate resting, and activated states of Kv7.1 generated from molecular dynamics simulations and Poisson-Boltzmann continuum electrostatic calculations. Red, E1; magenta, R1; cyan, R2; green, R3; blue, R4.

and tilts -20° about the transmembrane axis (Fig. 8 C). Although the accuracy of these simulated results is limited by the assumptions for constructing the homology model and the omission of interactions of S4 charges with lipid head groups (Schmidt et al., 2006; Xu et al., 2008), the model illustrates the mechanism as revealed by our experimental results. The electrostatic interactions between E1 and the arginines in S4 make energetic contributions to Kv7.1 gating and set the limits for the movement of the voltage sensor.

DISCUSSION

Our results show that E1 interacts electrostatically with S4 arginines during Kv7.1 activation. We can propose a mechanism by which the E1K mutation causes long QT syndrome. Mutating E1 to a positively charged residue repels S4 arginines to prevent S4 from moving to an activated conformation. This energetic blockade of S4 gating motion inhibits channels from opening and conducting current. Loss of I_{Ks} current reduces the total repolarizing current in the heart and prolongs the ventricular action potential, leading to long QT syndrome.

Kv7.1 has provided us with a unique opportunity to study electrostatic interactions between S2 and S4 in functional channels. In contrast to Shaker, in which charge reversal of E1 resulted in maturation-deficient channels (Tiwari-Woodruff et al., 1997), Kv7.1 was able to assemble and traffic to the membrane but could not conduct current. Thus, we were able to identify electrostatic interactions that are important for channel function. We performed paired charge reversal mutations to determine which mutant pairs could restore macroscopic current. Our hypothesis was that repulsion between a positive charge at E1 and positive charges in S4 inhibits channel opening by blocking S4 from moving to an activated state. Relieving repulsion and restoring attraction between specific pairs of residues may alleviate this energetic blockade, allowing S4 to move to an activated conformation and open channels. Using this charge reversal strategy, we identified that E1 interacts with R1–R4. We used other methods to more directly explore these interactions.

Once again, Kv7.1 provided us with a unique avenue to probe the electrostatic environment around E1. In Shaker, the E1C mutant produced low channel activity. Mutating R4Q in S4 with E1C restored channel activity and allowed modification by MTS reagents (Tiwari-Woodruff et al., 2000). However, the R4Q mutation may alter the electrostatic environment of E1C, allowing MTSET⁺ to modify E1C in addition to MTSES⁻, which prevents an effective means to probe the E1C electrostatic environment using MTS reagents. In our study, MTS reagents could not modify E1C in homomeric Kv7.1 channels; however, KCNE1 association exposed E1C to the extracellular solution, allowing access by

specific MTS reagents. We found that arginines in S4 create a positive electrostatic environment around E1C, which limited modification by positively charged MTS reagents. Because mutations reversing or neutralizing the charge at either R1 or R4 allow MTSET⁺ to approach and modify E1C, both R1 and R4 must affect the electrostatic environment of E1C. Unfortunately, we could not probe the influence of R2E/Q on E1C because these mutations remained constitutively open. Because R2 is positioned between R1 and R4, we reason that R2 also contributes to the electrostatic environment of E1.

Modification by MTSES⁻ and MTSET⁺ induces changes in the macroscopic current. For E1C/R1Q+KCNE1 and E1C/R1E/Q3R+KCNE1, modification by oppositely charged MTS reagents causes divergent effects: MTSET⁺ decreases current, whereas MTSES⁻ increases current. This result is consistent with the idea that a positive charge at E1 would attract R1E but repel other arginines in S4 (R2 and R4) to favor the resting state and prevent activation. On the other hand, a negative charge at E1 would form favorable electrostatic interactions with S4 arginines to facilitate activation. For E1C/R1E/Q3R+KCNE1, a negative charge at E1 would also repel R1E to destabilize the resting state.

For E1C/R4E+KCNE1, unmodified channels themselves behave very differently from native Kv7.1+KCNE1. Although E1C/R4E+KCNE1 activation is relatively normal, channels are extremely slow to deactivate, even at a holding potential of -80 mV for 32 s (Fig. 9 A). Because of this slow deactivation, open channels accumulate, resulting in an increase in the instantaneous current in subsequent pulses until channels reach equilibrium (Fig. 9 B). This result suggests that the mutation E1C/R4E may create a sterical hindrance for S4 to return to the resting state. After MTSET⁺ or MTSES⁻ modification, the charge at E1C is expected to interact with R1, R2, and R4E to increase or decrease channel activation, respectively. However, the results show that modification of E1C/R4E+KCNE1 by oppositely charged MTS reagent increases current, a phenomenon that cannot be simply explained by electrostatics. We do not completely understand the phenomenon, but one possible explanation is that the MTS compound attached

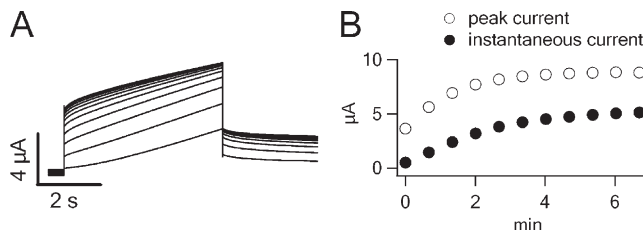


Figure 9. E1C/R4E+KCNE1 currents. (A) Oocytes were repeatedly depolarized to 40 mV for 5 s, repolarized at 40 mV for 3 s, and held at -80 mV for 32 s. (B) Time course of instantaneous and peak current after repeated pulses.

to E1C may alter the sterical hindrance of S4 movements, further preventing the voltage sensor from entering the resting conformation, thus increasing the number of open channels and increasing current.

Gating currents in Kv7.1 have never been recorded. This may be due to Kv7.1 carrying fewer S4 charges than other Kv channels, thus producing smaller gating currents. In addition, slow voltage sensor movements may also contribute to gating currents that are difficult to detect. Our study offers the first insight into the different conformational changes that S4 undergoes to become activated in Kv7.1. Although the voltage-dependent MTSET⁺ modification data obtained for E1C/R1E/Q3R with KCNE1 is measured at steady-state conditions and cannot directly report on a dynamic process, it is interesting to note that there appears to be three distinct and stable equilibrium states. The first two plateaus in the voltage dependence of rate of modification were left-shifted relative to the G-V relationship of this channel and correspond to the deep and intermediate resting states of S4, respectively (Fig. 8 B). At depolarizing potentials, S4 occupies a stable activated state. This implies that S4 moves in at least two distinct steps to reach the activated state, which is consistent with previous gating current and fluorescence experiments in Shaker and metal ion binding experiments in eag channels (Bezanilla et al., 1994; Baker et al., 1998; Silverman et al., 2003). Alternatively, the two-stage movement could be caused by rearrangements of other transmembrane segments besides S4. However, previous accessibility studies suggest that S4 undergoes the largest conformational changes during gating (Gandhi et al., 2003). Cysteine accessibility experiments in Kv7.1 show that residues at the top of S4, including R1, are more accessible at the activated state relative to the resting state (Nakajo and Kubo, 2007; Rocheleau and Kobertz, 2008). This rearrangement is consistent with our study in which R1 moves outward during activation from a position near E1 at rest. Collectively, our results indicate that arginines in S4 engage in electrostatic interactions with E1 in sequence during activation of the voltage sensor. This finding is consistent with recent disulfide cross-linking studies in a voltage-gated sodium channel (NaChBac) (DeCaen et al., 2008, 2009). The proposed interactions in these studies occur at different putative activated states. Our study provides evidence for an E1–R1 interaction at the resting state in addition to an E1–R4 interaction at the activated state of the Kv7.1 channel.

In conclusion, we found that E1 interacts electrostatically in a state-dependent manner with S4 arginines during activation. These electrostatic interactions contribute energetically to stabilizing S4 as it undergoes conformational changes within a hydrophobic lipid environment, helps guide its trajectory, and limits its movement during the gating process.

We thank S. Goldstein and S. Nakanishi for human KCNQ1 and KCNE1 clones, and H. Pan and X. Yang for preliminary mutagenesis.

This study was funded by an Established Investigator Award from the American Heart Association (AHA) and a research grant from the United States-Israel Binational Science Foundation to J. Cui; National Institutes of Health-National Heart, Lung and Blood Institute grants R01-HL49054 and R01-HL33343 to Y. Rudy; and AHA predoctoral fellowship 0910029G to D. Wu. J. Cui is the Associate Professor of Biomedical Engineering on the Spencer T. Olin Endowment, and Y. Rudy is the Fred Saigh Distinguished Professor of Engineering.

Christopher Miller served as editor.

Submitted: 29 January 2010

Accepted: 16 April 2010

REFERENCES

Aggarwal, S.K., and R. MacKinnon. 1996. Contribution of the S4 segment to gating charge in the Shaker K⁺ channel. *Neuron*. 16:1169–1177. doi:10.1016/S0896-6273(00)80143-9

Baker, O.S., H.P. Larsson, L.M. Mannuzzu, and E.Y. Isacoff. 1998. Three transmembrane conformations and sequence-dependent displacement of the S4 domain in shaker K⁺ channel gating. *Neuron*. 20:1283–1294. doi:10.1016/S0896-6273(00)80507-3

Barhanin, J., F. Lesage, E. Guillemaire, M. Fink, M. Lazdunski, and G. Romeo. 1996. K(V)LQT1 and IsK (minK) proteins associate to form the I(Ks) cardiac potassium current. *Nature*. 384:78–80. doi:10.1038/384078a0

Bezanilla, F., E. Perozo, and E. Stefani. 1994. Gating of Shaker K⁺ channels: II. The components of gating currents and a model of channel activation. *Biophys. J.* 66:1011–1021. doi:10.1016/S0006-3495(94)80882-3

Campos, F.V., B. Chanda, B. Roux, and F. Bezanilla. 2007. Two atomic constraints unambiguously position the S4 segment relative to S1 and S2 segments in the closed state of Shaker K channel. *Proc. Natl. Acad. Sci. USA*. 104:7904–7909. doi:10.1073/pnas.0702638104

DeCaen, P.G., V. Yarov-Yarovoy, Y. Zhao, T. Scheuer, and W.A. Catterall. 2008. Disulfide locking a sodium channel voltage sensor reveals ion pair formation during activation. *Proc. Natl. Acad. Sci. USA*. 105:15142–15147. doi:10.1073/pnas.0806486105

DeCaen, P.G., V. Yarov-Yarovoy, E.M. Sharp, T. Scheuer, and W.A. Catterall. 2009. Sequential formation of ion pairs during activation of a sodium channel voltage sensor. *Proc. Natl. Acad. Sci. USA*. 106:22498–22503.

Deng, C.X., F. Sieling, H. Pan, and J. Cui. 2004. Ultrasound-induced cell membrane porosity. *Ultrasound Med. Biol.* 30:519–526. doi:10.1016/j.ultrasmedbio.2004.01.005

Elinder, F., R. Männikkö, and H.P. Larsson. 2001. S4 charges move close to residues in the pore domain during activation in a K channel. *J. Gen. Physiol.* 118:1–10. doi:10.1085/jgp.118.1.1

Freites, J.A., D.J. Tobias, G. von Heijne, and S.H. White. 2005. Interface connections of a transmembrane voltage sensor. *Proc. Natl. Acad. Sci. USA*. 102:15059–15064. doi:10.1073/pnas.0507618102

Gandhi, C.S., E. Clark, E. Loots, A. Pralle, and E.Y. Isacoff. 2003. The orientation and molecular movement of a K(+) channel voltage-sensing domain. *Neuron*. 40:515–525. doi:10.1016/S0896-6273(03)00646-9

Haitin, Y., I. Yisharel, E. Malka, L. Shamgar, H. Schottelndreier, A. Peretz, Y. Paas, and B. Attali. 2008. S1 constrains S4 in the voltage sensor domain of Kv7.1 K⁺ channels. *PLoS One*. 3:e1935.

Hille, B. 2001. Ion Channels of Excitable Membranes, Third Edition. Sinauer Associates, Inc., Sunderland, MA. 814 pp

Krepkiy, D., M. Mihailescu, J.A. Freites, E.V. Schow, D.L. Worcester, K. Gawrisch, D.J. Tobias, S.H. White, and K.J. Swartz. 2009. Structure and hydration of membranes embedded with voltage-sensing domains. *Nature*. 462:473–479. doi:10.1038/nature08542

Larsson, H.P., O.S. Baker, D.S. Dhillon, and E.Y. Isacoff. 1996. Transmembrane movement of the shaker K⁺ channel S4. *Neuron*. 16:387–397. doi:10.1016/S0896-6273(00)80056-2

Lecar, H., H.P. Larsson, and M. Grabe. 2003. Electrostatic model of S4 motion in voltage-gated ion channels. *Biophys. J.* 85:2854–2864. doi:10.1016/S0006-3495(03)74708-0

Long, S.B., E.B. Campbell, and R. MacKinnon. 2005. Voltage sensor of Kv1.2: structural basis of electromechanical coupling. *Science*. 309:903–908. doi:10.1126/science.1116270

Long, S.B., X. Tao, E.B. Campbell, and R. MacKinnon. 2007. Atomic structure of a voltage-dependent K⁺ channel in a lipid membrane-like environment. *Nature*. 450:376–382. doi:10.1038/nature06265

Nakajo, K., and Y. Kubo. 2007. KCNE1 and KCNE3 stabilize and/or slow voltage sensing S4 segment of KCNQ1 channel. *J. Gen. Physiol.* 130:269–281. doi:10.1085/jgp.200709805

Nerbonne, J.M., and R.S. Kass. 2005. Molecular physiology of cardiac repolarization. *Physiol. Rev.* 85:1205–1253. doi:10.1152/physrev.00002.2005

Papazian, D.M., X.M. Shao, S.A. Seoh, A.F. Mock, Y. Huang, and D.H. Wainstock. 1995. Electrostatic interactions of S4 voltage sensor in Shaker K⁺ channel. *Neuron*. 14:1293–1301. doi:10.1016/S0896-6273(95)90276-7

Rocheleau, J.M., and W.R. Kobertz. 2008. KCNE peptides differently affect voltage sensor equilibrium and equilibration rates in KCNQ1 K⁺ channels. *J. Gen. Physiol.* 131:59–68. doi:10.1085/jgp.200709816

Sanguinetti, M.C., M.E. Curran, A. Zou, J. Shen, P.S. Spector, D.L. Atkinson, and M.T. Keating. 1996. Coassembly of K(V)LQT1 and minK (IsK) proteins to form cardiac I(Ks) potassium channel. *Nature*. 384:80–83. doi:10.1038/384080a0

Schmidt, D., Q.X. Jiang, and R. MacKinnon. 2006. Phospholipids and the origin of cationic gating charges in voltage sensors. *Nature*. 444:775–779. doi:10.1038/nature05416

Seoh, S.A., D. Sigg, D.M. Papazian, and F. Bezanilla. 1996. Voltage-sensing residues in the S2 and S4 segments of the Shaker K⁺ channel. *Neuron*. 16:1159–1167. doi:10.1016/S0896-6273(00)80142-7

Shi, J., G. Krishnamoorthy, Y. Yang, L. Hu, N. Chaturvedi, D. Harilal, J. Qin, and J. Cui. 2002. Mechanism of magnesium activation of calcium-activated potassium channels. *Nature*. 418:876–880. doi:10.1038/nature00941

Silva, J., and Y. Rudy. 2005. Subunit interaction determines IKs participation in cardiac repolarization and repolarization reserve. *Circulation*. 112:1384–1391. doi:10.1161/CIRCULATIONAHA.105.543306

Silva, J.R., H. Pan, D. Wu, A. Nekouzadeh, K.F. Decker, J. Cui, N.A. Baker, D. Sept, and Y. Rudy. 2009. A multiscale model linking ion-channel molecular dynamics and electrostatics to the cardiac action potential. *Proc. Natl. Acad. Sci. USA*. 106:11102–11106. doi:10.1073/pnas.0904505106

Silverman, W.R., B. Roux, and D.M. Papazian. 2003. Structural basis of two-stage voltage-dependent activation in K⁺ channels. *Proc. Natl. Acad. Sci. USA*. 100:2935–2940. doi:10.1073/pnas.0636603100

Splawski, I., J. Shen, K.W. Timothy, M.H. Lehmann, S. Priori, J.L. Robinson, A.J. Moss, P.J. Schwartz, J.A. Towbin, G.M. Vincent, and M.T. Keating. 2000. Spectrum of mutations in long-QT syndrome genes. KVLQT1, HERG, SCN5A, KCNE1, and KCNE2. *Circulation*. 102:1178–1185.

Tiwari-Woodruff, S.K., C.T. Schulteis, A.F. Mock, and D.M. Papazian. 1997. Electrostatic interactions between transmembrane segments mediate folding of Shaker K⁺ channel subunits. *Biophys. J.* 72:1489–1500. doi:10.1016/S0006-3495(97)78797-6

Tiwari-Woodruff, S.K., M.A. Lin, C.T. Schulteis, and D.M. Papazian. 2000. Voltage-dependent structural interactions in the Shaker K⁺ channel. *J. Gen. Physiol.* 115:123–138. doi:10.1085/jgp.115.2.123

Tombola, F., M.M. Pathak, and E.Y. Isacoff. 2006. How does voltage open an ion channel? *Annu. Rev. Cell Dev. Biol.* 22:23–52. doi:10.1146/annurev.cellbio.21.020404.145837

Xu, Y., Y. Ramu, and Z. Lu. 2008. Removal of phospho-head groups of membrane lipids immobilizes voltage sensors of K⁺ channels. *Nature*. 451:826–829. doi:10.1038/nature06618

Yang, N., A.L. George Jr., and R. Horn. 1996. Molecular basis of charge movement in voltage-gated sodium channels. *Neuron*. 16:113–122. doi:10.1016/S0896-6273(00)80028-8

Zagotta, W.N., T. Hoshi, and R.W. Aldrich. 1994. Shaker potassium channel gating. III: evaluation of kinetic models for activation. *J. Gen. Physiol.* 103:321–362. doi:10.1085/jgp.103.2.321

Zhang, L., Y. Sato, T. Hessa, G. von Heijne, J.K. Lee, I. Kodama, M. Sakaguchi, and N. Uozumi. 2007. Contribution of hydrophobic and electrostatic interactions to the membrane integration of the Shaker K⁺ channel voltage sensor domain. *Proc. Natl. Acad. Sci. USA*. 104:8263–8268. doi:10.1073/pnas.0611007104